

Effects of particle dipole interaction on the ac magnetically induced heating characteristics of ferrite nanoparticles for hyperthermia

Minhong Jeun, Seongtae Bae, Asahi Tomitaka, Yasushi Takemura, Ki Ho Park et al.

Citation: *Appl. Phys. Lett.* **95**, 082501 (2009); doi: 10.1063/1.3211120

View online: <http://dx.doi.org/10.1063/1.3211120>

View Table of Contents: <http://apl.aip.org/resource/1/APPLAB/v95/i8>

Published by the [American Institute of Physics](http://www.aip.org).

Related Articles

Fast switching of a ground state of a reconfigurable array of magnetic nano-dots

Appl. Phys. Lett. **100**, 192412 (2012)

Spatial control of magnetic anisotropy for current induced domain wall injection in perpendicularly magnetized CoFeB/MgO nanostructures

Appl. Phys. Lett. **100**, 192411 (2012)

Defect and adsorbate induced ferromagnetic spin-order in magnesium oxide nanocrystallites

Appl. Phys. Lett. **100**, 192404 (2012)

Measurement and simulation of anisotropic magnetoresistance in single GaAs/MnAs core/shell nanowires

Appl. Phys. Lett. **100**, 182402 (2012)

Formation and structure of colloidal halos in two-dimensional suspensions of paramagnetic particles

J. Chem. Phys. **136**, 164902 (2012)

Additional information on *Appl. Phys. Lett.*

Journal Homepage: <http://apl.aip.org/>

Journal Information: http://apl.aip.org/about/about_the_journal

Top downloads: http://apl.aip.org/features/most_downloaded

Information for Authors: <http://apl.aip.org/authors>

ADVERTISEMENT



Goodfellow
metals • ceramics • polymers • composites
70,000 products
450 different materials
small quantities fast

www.goodfellowusa.com

Effects of particle dipole interaction on the ac magnetically induced heating characteristics of ferrite nanoparticles for hyperthermia

Minhong Jeun,¹ Seongtae Bae,^{1,a)} Asahi Tomitaka,² Yasushi Takemura,² Ki Ho Park,³ Sun Ha Paek,⁴ and Kyung-Won Chung⁵

¹Department of Electrical and Computer Engineering, Biomagnetics Laboratory (BML), National University of Singapore, Singapore 117576, Singapore

²Department of Electrical and Computer Engineering, Yokohama National University, Yokohama 240-8501, Japan

³Department of Ophthalmology, Seoul National University College of Medicine, Seoul 110-744, Republic of Korea

⁴Department of Neurosurgery, Seoul National University College of Medicine, Seoul 110-744, Republic of Korea

⁵Daion Co. Ltd., Incheon 405-846, Republic of Korea

(Received 1 July 2009; accepted 30 July 2009; published online 24 August 2009)

Magnetic particle dipole interaction was revealed as a crucial physical parameter to be considered in optimizing the ac magnetically induced heating characteristics of magnetic nanoparticles. The ac heating temperature of soft $M\text{Fe}_2\text{O}_4$ ($M=\text{Mg},\text{Ni}$) nanoparticles was remarkably increased from 17.6 to 94.7 °C (MgFe_2O_4) and from 13.1 to 103.1 °C (NiFe_2O_4) by increasing the particle dipole interaction energy at fixed ac magnetic field of 140 Oe and frequency of 110 kHz. The increase in “magnetic hysteresis loss” that resulted from the particle dipole interaction was the main physical reason for the significant improvement of ac heating characteristics. © 2009 American Institute of Physics. [DOI: 10.1063/1.3211120]

Hyperthermia therapy using a magnetic nanoparticle agent, a modality of cancer treatment with an elevated temperature of 43–45 °C with treating time over 30 min, has recently drawn huge attention due to its clinical promise.^{1,2} However, for the practical use of this modality in real clinics, magnetic nanoparticle agents should satisfy a few of technical requirements such as a high enough ac magnetically induced heating temperature ($\Delta T_{\text{ac,mag}}$), a high specific absorption rate (SAR), an injection through blood vessels without any clotting problems, and a high biocompatibility in living cells.³ Among these technical limits, the sufficiently high $\Delta T_{\text{ac,mag}}$ and SAR at a small particle concentration are considered as the most critical challenges to achieve a reliable tumor damage and no recurrence for the clinical hyperthermia with a good prognosis.⁴ Especially, considering a temperature reduction due to a blood circulation and a tissue perfusion in an *in vivo* environment, the solid state magnetic nanoparticles should produce a sufficiently high $\Delta T_{\text{ac,mag}}$ in the range of 60–80 °C with a SAR as high as possible in the physiologically tolerable range of the applied frequencies and magnetic fields [$f \sim 100$ kHz and $H \sim 15$ kA/m ($H_0 \cdot f = 4.85 \times 10^8$ A/m s)].⁵

It is well known that the “magnetic hysteresis loss” and the “relaxation loss” are primarily responsible for the physical mechanism of $\Delta T_{\text{ac,mag}}$ of the magnetic nanoparticles.⁶ Particularly, since the contribution of the magnetic hysteresis loss to the $\Delta T_{\text{ac,mag}}$ has been confirmed more dominant in ferrimagnetic nanoparticles,⁷ research efforts to improve the $\Delta T_{\text{ac,mag}}$ /SAR of magnetic nanoparticles have been intensively focused on increasing the magnetic hysteresis loss, e.g., controlling both magnetic susceptibility ($\chi_m = \chi'_m + i\chi''_m$) and magnetic moment [$M = \chi_m H = (\chi'_m + i\chi''_m)H$] of existing

magnetic nanoparticles as well as developing soft magnetic particles.^{8,9} From this physical viewpoint, controlling magnetic dipole interaction formed among the magnetic nanoparticles can be an approach to enhance the magnetic hysteresis loss because the particle dipole interaction would directly influence the variation in magnetic susceptibility and moment of magnetic nanoparticles.¹⁰ However, although this physical phenomenon is theoretically considered to improve the magnetic hysteresis loss and effectively control the magnetic properties of magnetic nanoparticles, there has been no empirical demonstration on the effects of particle dipole interaction on the ac magnetically induced heating characteristics, $\Delta T_{\text{ac,mag}}$ /SAR, of magnetic nanoparticles so far.

In this letter, we demonstrate the effects of particle dipole interaction on the ac magnetically induced heating characteristics of soft (Mg, Ni) and hard (Co) $M\text{Fe}_2\text{O}_4$ ferrimagnetic nanoparticles. The correlation between the physical nature of particle dipole interaction and the ac magnetically induced heating characteristics was interpreted in terms of the variation in magnetic susceptibility, magnetic moment, and magnetic hysteresis (and minor hysteresis) behavior depending on the degree of particle dipole interaction. The particle dipole interaction of the $M\text{Fe}_2\text{O}_4$ nanoparticles was controlled by varying the size distribution of the nanoparticles.

The spinel ferrite $M\text{Fe}_2\text{O}_4$ ($M=\text{Mg},\text{Ni},\text{Co}$) nanoparticles with 30–33 nm mean particle sizes were prepared by using a sol-gel method. The size distribution of the nanoparticles was systematically controlled from 22.1% to 59.3% in standard deviation (Sdv.) by using acidic solvents in the sol-gel process and changing the ramping rate of temperature in the sintering process. The size and distribution of $M\text{Fe}_2\text{O}_4$ nanoparticles were determined by field emission scanning electron microscopy (FE-SEM), as shown in Fig. 1. The magnetic hysteresis (M - H) loops and the $\Delta T_{\text{ac,mag}}$ characteristics were measured by using a vibrating sample magneto-

^{a)}Electronic mail: elebst@nus.edu.sg.

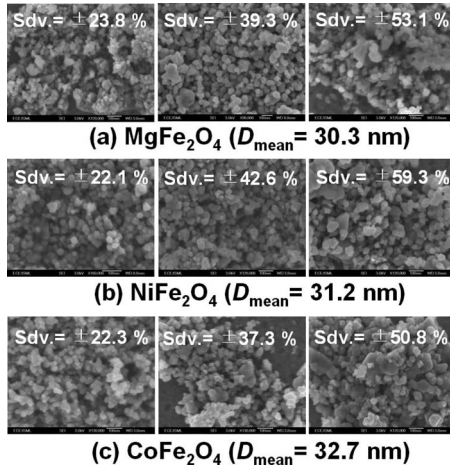


FIG. 1. FE-SEM images of (a) MgFe_2O_4 , (b) NiFe_2O_4 , and (c) CoFe_2O_4 nanoparticles with different particle size distributions.

meter and a specially designed rf-induced LC coil, respectively.⁷ The applied ac magnetic field H_{appl} and the frequency f_{appl} during the temperature measurement were varied from 50 to 140 Oe and from 40 to 210 kHz, respectively. The SAR was determined from the experimentally obtained heating temperature.

Figure 2 shows the dependence of particle size distribution of $M\text{Fe}_2\text{O}_4$ nanoparticles on the $\Delta T_{\text{ac,mag}}$ characteristics measured at fixed $H_{\text{appl}}=140$ Oe and $f_{\text{appl}}=110$ kHz. As can be clearly seen in Fig. 2, the maximum $\Delta T_{\text{ac,mag}}$ of soft $M\text{Fe}_2\text{O}_4$ nanoparticles were remarkably increased from 17.6 to 94.7 °C (Sdv.: from 23.8% to 53.1%) for MgFe_2O_4 and from 13.1 to 103.1 °C (Sdv.: from 22.1% to 59.3%) for NiFe_2O_4 , respectively. However, the hard CoFe_2O_4 nanoparticles had no dependence of particle size distribution on the $\Delta T_{\text{ac,mag}}$. The physical reason for the significant increase in $\Delta T_{\text{ac,mag}}$ with increasing particle size distribution can be elucidated by considering the physical correlation between the magnetic properties and the magnetic particle dipole interaction. Figure 3 shows a schematic diagram of our model for the particle dipole interaction. The particle dipole interaction energy E_{int} can be expressed by¹¹

$$E_{\text{int}} = \frac{m_1 m_2}{r^3} [\cos(\theta_1 - \theta_2) - 3 \cos \theta_1 \cos \theta_2], \quad (1)$$

where r is a distance between centers of the neighboring nanoparticles with magnetic moments m_1 and m_2 , and θ_1 and

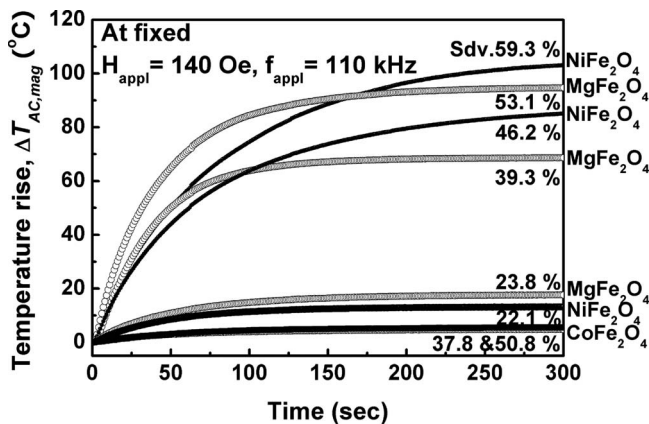


FIG. 2. Dependence of the particle size distribution on the ac magnetically induced heating characteristics of MgFe_2O_4 , NiFe_2O_4 , and CoFe_2O_4 nanoparticles measured at fixed $H=140$ Oe and $f=110$ kHz.

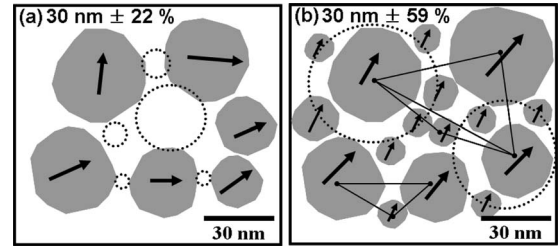


FIG. 3. The schematic diagrams illustrating the magnetization of particles induced by different particle dipole interactions. The particle size and its distribution were approximately assumed as (a) $30 \text{ nm} \pm 22\%$ and (b) $30 \text{ nm} \pm 59\%$.

θ_2 are angles between the magnetization directions and a vector joining them. Assuming that the adjacent magnetizations of nanoparticles are in parallel or the magnetization angle difference is negligibly small under the ac magnetic field (or magnetic reversal more coherently), Eq. (1) can be simplified by

$$E_{\text{int}} = \frac{m_1 m_2}{r^3} [1 - 3 \cos^2 \theta]. \quad (2)$$

In the case of narrow size distribution [Fig. 3(a)], the large particle gaps created among the neighboring nanoparticles cause the distance r between the adjacent nanoparticles to increase, leading to a relatively weak particle dipole interaction resulting in a small E_{int} and correspondingly a small exchange coupling energy J_{ex} among the nanoparticles.⁹ This induces a relatively less coherent magnetization reversal as well a relatively longer spin relaxation under the ac applied field. However, in the case of wide size distribution [Fig. 3(b)], the particle gaps would be possibly filled with small size nanoparticles (negative Sdv.) that can be interparticle bridged to increase both E_{int} and J_{ex} among the nanoparticles.¹⁰ This leads to induce a relatively more coherent magnetization reversal as well a relatively shorter spin relaxation under the ac applied field. Moreover, the additionally increased J_{ex} attributed to the enhanced E_{int} allows to increase the total magnetic moment, $m_{\text{tot}}=m_1+m_2+\Delta m_1 m_2$, as well the magnetic susceptibility. Consequently, a larger magnetic hysteresis loss and an improved relaxation loss, especially “Néel relaxation loss” would be expected to result in enhancing the ac magnetically induced heating characteristics. This physical assumption was confirmed by analyzing the magnetic behavior of $M\text{Fe}_2\text{O}_4$ ($M=\text{Mg}, \text{Ni}, \text{Co}$) nanoparticles, as shown in Fig. 4. By increasing the particle dipole interaction (particle size distribution), the saturation magnetization of $M\text{Fe}_2\text{O}_4$ nanoparticles was prominently increased [Figs. 4(a), 4(c), and 4(e)] and the initial magnetic susceptibility was correspondingly increased [upper insets in Figs. 4(a), 4(c), and 4(e)]. In addition, the gentle slope of M - H loops ($\Delta M/\Delta H$) and the increased magnetic coercivity [lower insets in Figs. 4(a), 4(c), and 4(e)] obviously obtained from the nanoparticles with narrow size distribution indicate that the particle dipole interaction is directly relevant to the magnetic properties of $M\text{Fe}_2\text{O}_4$ nanoparticles. This physical phenomenon was found more obvious for the soft (Mg, Ni) $M\text{Fe}_2\text{O}_4$ nanoparticles than for the hard (Co) magnetic nanoparticles because the CoFe_2O_4 nanoparticles have a higher magnetic anisotropy. Figures 4(b), 4(d), and 4(f) show the minor M - H loops measured at the applied magnetic field of ± 140 Oe. As can be clearly confirmed, the “minor hysteresis

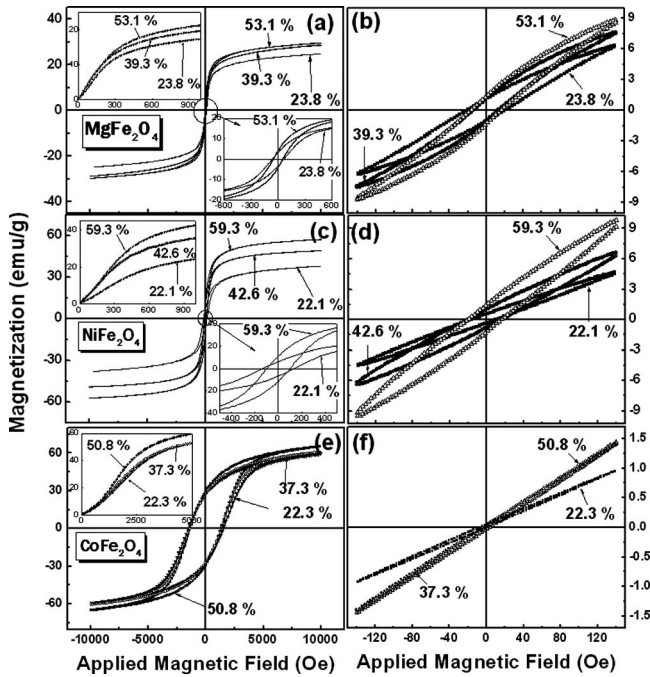


FIG. 4. M - H loops, initial M - H curves, and minor hysteresis loops of $M\text{Fe}_2\text{O}_4$ nanoparticles with different particle size distributions: [(a) and (b)] MgFe_2O_4 , [(c) and (d)] NiFe_2O_4 , and [(e) and (f)] CoFe_2O_4 .

area (loss)” was proportionally increased by increasing the particle size distribution (or particle dipole interaction). This directly demonstrates that the increased particle dipole interaction induces a larger magnetic hysteresis loss, which is the main physical reason for the remarkably increased $\Delta T_{ac,mag}$. The effects of particle dipole interaction on the ac magnetically induced heating characteristics were also analyzed by evaluating the variation in SAR depending on the particle size distribution, as shown in Fig. 5. The SAR was determined from the measured heating temperature using¹²

$$\text{SAR} = \frac{\sum_i C_i \times m_i \Delta T}{m_{M\text{Fe}_2\text{O}_4} \Delta t} \quad (\text{W/g}), \quad (3)$$

where C_i is the volumetric heat capacity, m_i is the mass of each component in the system, $m_{M\text{Fe}_2\text{O}_4}$ is the mass of the each ferrimagnetic nanoparticle (60 mg), and ΔT and Δt are the 63% change in temperature at T_{max} and the corresponding

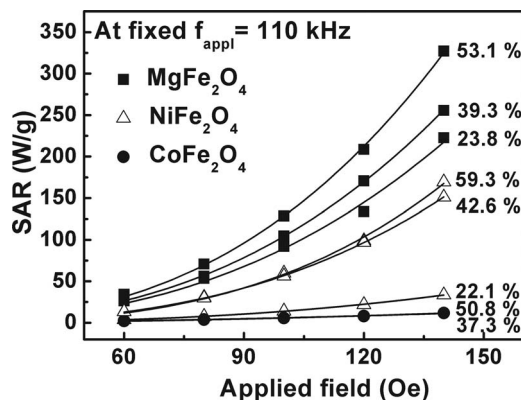


FIG. 5. SAR of $M\text{Fe}_2\text{O}_4$ nanoparticles with different size distributions determined at the different ac magnetic fields.

change in time, respectively. It was found that the SAR of soft (Mg, Ni) $M\text{Fe}_2\text{O}_4$ nanoparticles was squarely proportional to the applied ac magnetic field. Particularly, the SAR had a strong dependence on the particle size distribution, indicating that the increase in $\Delta T_{ac,mag}$ controlled by the particle dipole interaction is directly responsible for the significant increase in SAR. The SAR was increased up to a 327.2 W/g (Sdv.: 53.1%) for MgFe_2O_4 nanoparticles and a 169.4 W/g (Sdv.: 59.3%) for NiFe_2O_4 nanoparticles, respectively. The hard CoFe_2O_4 nanoparticle showed an extremely low SAR due to its high magnetic anisotropy. However, as interestingly noted in Fig. 5, despite the highest $\Delta T_{ac,mag}$, NiFe_2O_4 nanoparticles (Sdv.: 59.3%) had a much lower SAR than that of MgFe_2O_4 nanoparticles (Sdv.: 53.1%). This can be taken into account by considering the “thermal conductivity, σ_{th} ,” which is directly proportional to the electrical conductivity.¹³ The NiFe_2O_4 nanoparticles have a higher electrical conductivity ($\sim 10^{-5}$ S/cm) than that of MgFe_2O_4 ($\sim 10^{-7}$ S/cm) nanoparticles.¹⁴ The higher thermal conductivity gives rise to a faster heat dissipation (or larger heat loss) during the ac magnetically induced heating, thus a longer time (Δt) is required to reach 63% of T_{max} . The gentle slope ($\Delta T/\Delta t$) of NiFe_2O_4 nanoparticles shown in Fig. 2 is agreed well with the lower SAR of NiFe_2O_4 nanoparticles.

In conclusion, the $\Delta T_{ac,mag}/\text{SAR}$ of soft $M\text{Fe}_2\text{O}_4$ (Mg, Ni) nanoparticles was remarkably increased by controlling the particle dipole interaction. According to the magnetic analysis results, the huge enhancement of $\Delta T_{ac,mag}/\text{SAR}$ was found to be primarily due to the increase in magnetic hysteresis loss and relaxation loss resulted from the increase in magnetic moment and susceptibility induced by the particle dipole interaction energy. All the experimental results in this work clearly demonstrate that the particle dipole interaction formed among the nanoparticles should be considered as one of the most crucial physical parameters in optimizing the magnetic and ac magnetically induced heating characteristics of nanoparticles for a hyperthermia agent application.

¹R. K. Gilchrist, R. Medal, W. D. Shorey, R. C. Hanselman, J. C. Parrott, and C. B. Taylour, *Ann. Surg.* **146**, 596 (1957).

²P. Moroz, S. K. Jones, and B. N. Gray, *Int. J. Hyperthermia* **18**, 267 (2002).

³Q. A. Pankhurst, J. Connolly, S. K. Jones, and J. Dobson, *J. Phys. D* **36**, R167 (2003).

⁴J. R. Oleson, R. S. Heusinkveld, and M. R. Manning, *Int. J. Radiation Oncology, Biol., Phys.* **9**, 549 (1983).

⁵A. Jordan, R. Scholz, P. Wust, H. Föhling, and R. Felix, *J. Magn. Magn. Mater.* **201**, 413 (1999).

⁶R. E. Rosensweig, *J. Magn. Magn. Mater.* **252**, 370 (2002).

⁷S. Bae, S. W. Lee, A. Hirukawa, Y. Takemura, Y. H. Jo, and S. G. Lee, *IEEE Trans. Nanotechnol.* **8**, 86 (2009).

⁸P. C. Fannin and S. W. Charles, *J. Phys. D: Appl. Phys.* **24**, 76 (1991).

⁹T. Maehara, K. Konishi, T. Kamimori, H. Aono, H. Hirazawa, T. Naohara, S. Nomura, H. Kikkawa, Y. Watanabe, and K. Kawachi, *J. Mater. Sci.* **40**, 135 (2005).

¹⁰P. Poddar, T. T. Shafir, T. Fried, and G. Markovich, *Phys. Rev. B* **66**, 060403 (2002).

¹¹I. S. Jacobs and C. P. Bean, *Phys. Rev.* **100**, 1060 (1955).

¹²T. Hosono, H. Takahashi, A. Fujita, R. J. Joseyphus, K. Tohji, and B. Jeyadevan, *J. Magn. Magn. Mater.* **321**, 3019 (2009).

¹³M. William and H. Norman, *Theoretical Solid State Physics* (Courier Dover, New York, 1985).

¹⁴A. Goldman, *Modern Ferrite Technology* (Springer, New York, 2006).